This is an *Accepted Manuscript*, which has been through the RSC Publishing peer review process and has been accepted for publication.

Accepted Manuscripts are published online shortly after acceptance, which is prior to technical editing, formatting and proof reading. This free service from RSC Publishing allows authors to make their results available to the community, in citable form, before publication of the edited article. This *Accepted Manuscript* will be replaced by the edited and formatted *Advance Article* as soon as this is available.

To cite this manuscript please use its permanent Digital Object Identifier (DOI®), which is identical for all formats of publication.

More information about *Accepted Manuscripts* can be found in the **Information for Authors**.

Please note that technical editing may introduce minor changes to the text and/or graphics contained in the manuscript submitted by the author(s) which may alter content, and that the standard **Terms & Conditions** and the **ethical guidelines** that apply to the journal are still applicable. In no event shall the RSC be held responsible for any errors or omissions in these *Accepted Manuscript* manuscripts or any consequences arising from the use of any information contained in them.

High performance Pd nanocrystals supported on SnO$_2$-decorated graphene for aromatic nitro compound reduction

Hongyan Li, [a,b] Shiyu Gan, [a,b] Dongxue Han,*[a] Weiguang Ma, [a,b] Bin Cai, [a,b] Wei Zhang, [a,b] Qixian Zhang, [a] and Li Niu[a]

[a] *State Key Laboratory of Electroanalytical Chemistry, c/o Engineering Laboratory for Modern Analytical Techniques, Changchun Institute of applied Chemistry, Chinese Academy of Sciences, Changchun, 130022, Jilin, China,. Fax: +8643185262800; Tel: +8643185262425; E-mail: dxhan@ciac.ac.cn*

[b] *University of Chinese Academy of Sciences, Beijing 100039, China*
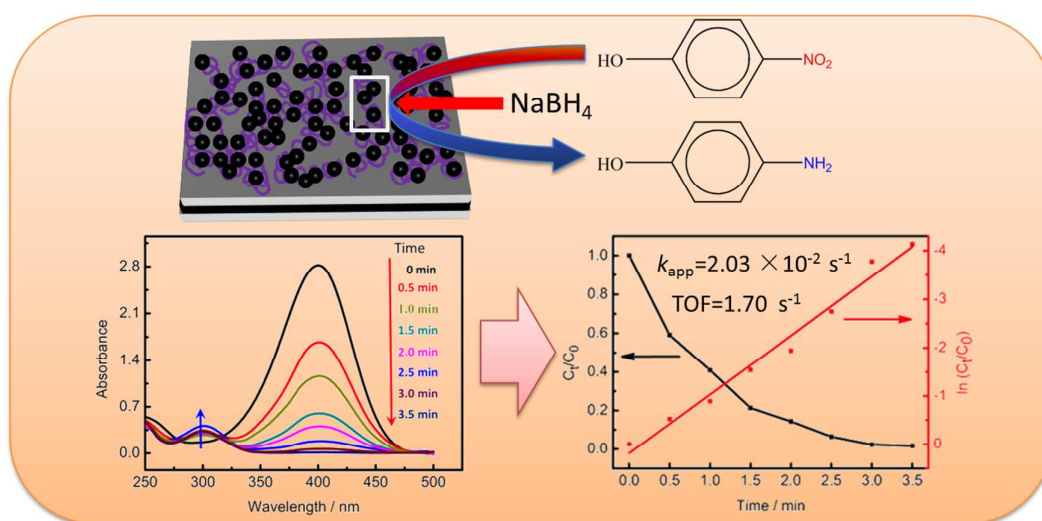
We reported a hybrid material of ultrafine Pd nanocrystals (PdNCs) grown on an excellent support of SnO$_2$-decorated graphene nanosheets (SnO$_2$-GNS) for a high efficient reduction of a representative aromatic nitro compound (4-nitrophenol).

ARTICLE TYPE

High performance Pd nanocrystals supported on SnO₂-decorated graphene for aromatic nitro compound reduction

Hongyan Li, [a,b] **Shiyu Gan,** [a,b] **Dongxue Han,*** [a] **Weiguang Ma,** [a,b] **Bin Cai,** [a,b] **Wei Zhang,** [a,b] **Qixian Zhang,** [a] **and Li Niu** [a]

Promotion of the catalytic efficiency and reduction of the usage amount of Pd are crucial to developing effective and low-cost catalysts for catalytic reduction of organic aromatic nitro pollute compound at present. Herein, we report a hybrid material of ultrafine Pd nanocrystals (PdNCs) grown on excellent
10 support of SnO₂-decorated graphene nanosheets (SnO₂-GNS) for a high efficient reduction of a representative aromatic nitro compound (4-nitrophenol). The supported material of SnO₂-GNS was simply prepared by one step of homogeneous reaction with a positive charged polymer as stabilizer and active site for absorption of PdNCs precursor. Transmittance electronic images demonstrate that the PdNCs are densely and well covered on the SnO₂-GNS with a uniform size of 3.4 nm. This nanohybrid
15 exhibits the fastest reduction time (4 minutes) compared to other controlled materials. Moreover, it shows high kinetic responses with the apparent kinetic rate constant (k_{app}) of 2.03×10^{-2} s⁻¹ and turnover frequency (TOF) of 1.70 s⁻¹. The cycle performance (10 times) experiments demonstrate that this nanohybrid also displays a good anti-poisoning capability. Thanks to the ultrafine PdNCs, this as-prepared PdNCs/SnO₂-GNS nanohybrid may have broad potentials in other catalytic fields, for example,
20 organic synthesis, fuel cell and electrochemical biosensors.

1. Introduction

Organic aromatic nitro compounds are widely generated as by-products in different industries and agriculture,[1, 2] such as colouring agents, agrochemicals and pharmaceutical products.[3]
25 Among various aromatic nitro compounds, 4-nitrophenol (4-NP) is one of the mostly produced by-products,[4] which is contaminant to the environment. In pharmaceutical industries, 4-aminophenol (4-AP) is always derived from 4-NP by reduction. The 4-AP is well known as a vital precursor for the production of various
30 medicines like paracetamol, phenacetin, acetanilide and antipyretic drugs etc.[5] It is also widely developed as photographic developer, corrosion inhibitor, anticorrosion-lubricant and hair-dyeing agent.[6] Based on this fact, it is necessary to catalyze reduction of 4-NP into 4-AP, which can not only reduce the
35 pollution of the environment but also make waste into treasure.

The noble metal Pd NCs catalyst has attracted intensively attention due to its unique physical and chemical properties.[7, 8] It has significant applications from catalysis for Suzuki coupling reactions[7, 9] to hydrogen sensors,[10] energy storage,[11-13] fuel
40 cells[14-17] and the degradation of pollutants.[18-20] It is also worth pointing out that the reduction of 4-NP over noble metal nanocatalyst, especially the Pd nanocatalysts, has been interestingly investigated for efficient production of 4-AP in the presence of NaBH₄.[21] For example, Morère et al.[22] reported a
45 mild strategy to synthesis mesoporous silica SBA-15 as the support of Pd NCs as an advanced catalyst material for reduction

of 4-NP to 4-AP. The immobilization of Pd NCs on alumina (Al₂O₃) as a new catalyst through a simple physical precipitation method has been reported by Shailja Arora[23] for the industrially
50 reduction of aromatic nitro compounds to amino compounds. Although these large size Pd-based catalysts can well catalyze reduction of 4-NP to 4-AP, the catalytic efficiency still needs to be improved in the commercial field. As is known that, the catalytic performance of the Pd nanocatalyst greatly depends on
55 two factors: (1) the particle size; (2) the dispersion of Pd NCs in the materials. Smaller sizes of Pd NCs will significantly enhance the surface-to-volume ratio, which leads to the further improvement of catalytic performance.[24] However, the surface energy also increases when the nanoparticle size decreases, which
60 usually leads to serious aggregation problem.[25, 26] Therefore, it remains a major challenge how to improve the stability, recyclability and catalytic activity of Pd NCs. For this purpose, it is necessary to load Pd NCs on the surface of supporting materials with low cost, high surface area, excellent chemical and
65 physical properties, such as metal oxides,[24, 26] carbon,[27, 28] polymers,[29] and so on.

In this paper, we introduced SnO₂-GNS as a new kind of building block material due to their excellent synergistic effects.[30-32] SnO₂-decorated GNS was treated with poly
70 (diallyldimethylammonium chloride) (PDDA), which would provide many positive charged active sites. Meanwhile, the SnCl₂ • 2H₂O was added into the solution to act as both the reducing agent for GNS and the precursor of SnO₂. SnO₂-GNS

not only provide a platform for self-assembly the Pd NCs by electrostatic adsorption, but also prevent Pd NCs aggregation. Furthermore, it was found that the as-prepared PdNCs/SnO$_2$-GNS nanohybrid exhibited highly efficient activity as catalyst for reduction of 4-NP to 4-AP by NaBH$_4$. In addition, other previously reported Pd-based catalysts[22, 23, 25, 33-36] have also been compared with our PdNC/SnO$_2$-GNS hybrid. The results distinctly show that, the as-synthesized PdNC/SnO$_2$-GNS exhibit preferable catalytic efficiency. And the kinetic apparent rate constant (k_{app}) and turnover frequency (TOF) of PdNC/SnO$_2$-GNS reach about 2.03×10^{-2} s^{-1} and 1.70 s^{-1}, respectively, which demonstrate great potential in the commercial applications.

2. Experimental section

2.1 Chemicals

Sodium tetrachloropalladate (II) (Na$_2$PdCl$_4$ 99.9%) and poly (diallyldimethylammonium chloride) (PDDA, 20 wt.% in water) were purchased from Sigma-Aldrich. p-nitrophenol was obtained from Aladdin. Graphite powder (325 mesh), sodium borohydride (NaBH$_4$), Tin (II) chloride dehydrate (SnCl$_2$·2H$_2$O), HCl (36-38%) were purchased from Beijing Chemical Factory (Beijing, China). All chemicals were used as received without further purification. All aqueous solutions were prepared with ultra-pure water (>18 MΩ) from a Milli-Q Plus system (Millipore). All glasswares used in the following procedures were cleaned in a bath of freshly prepared HCl: HNO$_3$ (3: 1, aqua regia) and rinsed thoroughly with water prior to use.

2.2 Preparation of graphene oxide (GO)

Graphene oxide (GO) was prepared by oxidizing natural graphite power based on a modified Hummers method.[37] GO was then suspended in ultra-pure water to form a brown dispersion, which was further treated by dialysis for 6-7 days to completely remove metal ions and acids.[38], The concentration of finally obtained GO product was calibrated with the UV-Vis spectra at room temperature.

2.3 Preparation of PDDA-functionalized SnO$_2$-GNS

SnO$_2$-GNS was synthesized according to previous work with minor modifications.[30, 39] Briefly，20 mL GO (0.5 mg mL^{-1}) and 0.5 mL PDDA were mixed in a round bottom flask and stirred for more than 30 minutes. Subsequently, 0.15 mL of HCl, 0.30 g of SnCl$_2$·2H$_2$O were added. The mixture was then continually stirred at 90 ℃ for 3 h. After the mixture was cooled to ambient temperature, it was centrifuged and washed with ultra-pure water for three times. Finally, the obtained SnO$_2$-GNS was dispersed into 50 mL water for further use. As control, SnO$_2$-GNS nanocomposites were prepared under the same conditions without introducing of PDDA.

2.4 Preparation of PdNCs/SnO$_2$-GNS nanohybrid materials

1mL of Na$_2$PdCl$_4$ aqueous solution (5mM) and as-prepared 20 mL SnO$_2$-GNS dispersion were mixed together while stirring for more than about 60 minutes. Then 1mL of NaBH$_4$ (5.63 mg) was added into the above mixture. It was stored at room temperature for several hours until the PdCl$_4^{2-}$ was completely reduced. The solution was then centrifuged and washed with ultra-pure water for three times. Finally, the obtained PdNCs/SnO$_2$-GNS

Graphene oxide　PDDA　SnO$_2$　PdCl$_4^{2-}$　Graphene　Pd NP
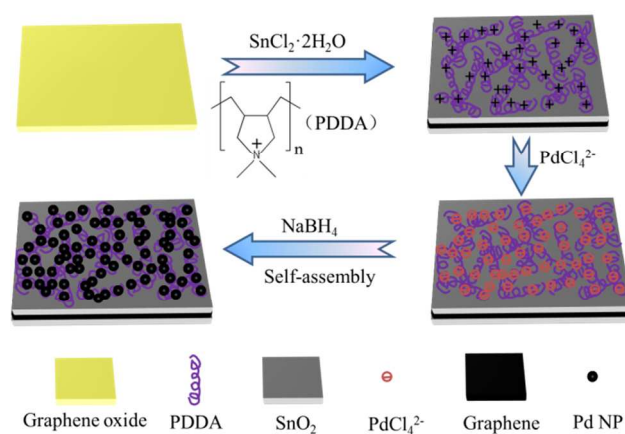
Scheme 1 Procedure to synthesis Pd NCs supported on SnO$_2$-decorated graphene nanohybrid material

nanohybrid was dispersed in 20 mL water for further experiment.

2.5 Catalytic studies

In order to investigate the catalytic activity of as-prepared PdNCs/SnO$_2$-GNS, freshly prepared 50 μL of 4-NP solution (10 mM) and 50 μL of NaBH$_4$ solution (3 M) were added into a quartz cuvette and the color of reaction system were observed to transfer from light yellow to yellow-green. Then 3 mL of aqueous solution containing 5 μL PdNCs/SnO$_2$-GNS nanohybrid was injected into the cuvette which started the reaction. The change of the intensity of the absorption peak at 400 nm of 4-NP was monitored by UV-vis spectroscopy as function of reduction time. When the solution became colorless, it indicated the accomplishment of the reaction. Afterwards, another 100 μL of mixed reagent of 4-NP (10 mM) and NaBH$_4$ (3 M) was added into the reaction system after each round of reaction. This step was repeated nine rounds to study the stability of catalyst.

2.6 Instrumentation

Ultraviolet-Visible (UV-Vis) absorption spectra were recorded with a U-3900 of HITACHI UV-Vis spectrophotometer. Transmission electron microscopy (TEM) images were carried out on a Hitachi-600 TEM with an accelerating voltage of 100 kV. The samples for TEM images were prepared by dropping the dilute colloidal suspension (~0.05 mg mL^{-1}) onto a carbon-covered copper grid and dried in air at ambient temperature. High-resolution transmission electron microscopy (HRTEM) and energy dispersive X-ray spectroscopy (EDX) measurements were performed on a Tecnai G^2 microscope at 200 kV. The X-ray photoelectron spectroscopy (XPS) analysis was performed on an ESCALAB-MKII X-ray photoelectron spectrometer (VG Co.) with Al Kα X-rays radiation as the X-ray source for excitation. Fourier transform infrared spectra (FTIR) were collected on a Bruker Tensor 27 spectrometer. Zeta potential measurements were performed using a Zetasizer NanoZS (Malvern Instruments). Atomic force microscopy (AFM) images were obtained with Veeco Instruments Nanoscope in tapping mode. The samples for AFM measurements were prepared by dropping the diluted colloidal suspension (~0.01 mg mL^{-1}) onto a freshly cleaved mica surface and then dried in air. The weight of the Pd in the PdNCs/SnO$_2$-GNS nanohybrid was determined by inductively coupled plasma (ICP) atomic emission spectrometric analysis.

3. Results and discussion

3.1 Characterization of Materials

A well-dispersed GO with nanosheet structure was synthesized by the modified Hummers method in this study, which provides a raw material as building block to self-assembly the metal nanoparticles. As shown in **Scheme 1**, PdNCs/SnO₂-GNS nanohybrid was generated by *in situ* reduction of negatively charged $PdCl_4^{2-}$ precursors adsorbed on the positively charged surface of SnO₂-GNS through electrostatic attraction. Here, $SnCl_2$ not only acts as the reducing agent for GO, but also the precursor of SnO_2. **Fig.1a** and **1b** are the typical TEM images of prepared GO and SnO₂-GNS nanocomposites, respectively. It clearly shows that the as-obtained GO exhibits the appearance of a wrinkle-like thin sheet, which is the feature structure of GO nanosheets[31]. While SnO₂-GNS nanocomposites present well-defined nanofilm morphology.[39, 40]
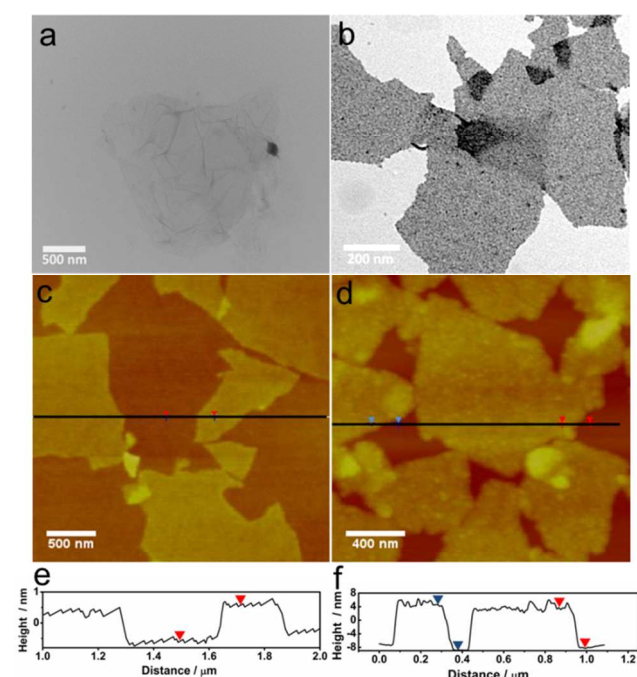
Fig.1 TEM, AFM image of GO (a, c) and the SnO₂-decorated GNS (b, d) and their height profiles (e, f), respectively.

At the same time, in order to prove that the SnO_2 was decorated on both sides of the GNS and uniform plane of nanoparticles has formed. Further investigation by atomic force microscopy (AFM) analysis has also been performed. **Fig.1c** and **1d** are the typical images of AFM of GO and SnO₂-GNS nanocomposites, respectively. It reveals that SnO_2, as the templates, were uniformly decorated on GNS. The height profile of GO is about 0.9 nm (**Fig.1e**), which is similar to the original GO properties just as reported.[41, 42] The average thickness of SnO₂-GNS is found to be ~12.5 nm (**Fig.1f**) due to formation of SnO_2 and introduction of PDDA. All of the results shown in **Fig.1** reveals that the introduction of PDDA does not change the morphology of GO.[17,43,44] PDDA plays significant role for providing the positive charge site to attract the negatively charged $PdCl_4^{2-}$ ions *via* the electrostatic interactions. And Pd NCs with small size of 3.4 nm were directly self-assembly on both sides of

the SnO₂-GNS nanocomposites upon the redox reaction.

In order to assess the reduction of GO and formation of SnO₂-GNS, UV-vis absorption spectra (**Fig.S1**) and FT-IR spectra (**Fig.S2**) were recorded. The UV-vis characteristic absorption peak of GO at 230 nm disappeared and red shifted to a broad peak located at 260 nm, which indicated the reduction of GO. [40, 45] In addition, the absence of the peaks at 1730 cm⁻¹ (C=O) and 1421 cm⁻¹ (C–OH) indicated the removal of oxygen containing groups from GO after reduction.[45] The appeared absorption peaks at 1629 cm⁻¹ (C=C) and 1460 cm⁻¹ are found to be characteristic absorption peaks of PDDA.[46]

Results of the above characterizations clearly show that SnO_2 has been successfully decorated on the surface of the GNS, which exhibit an excellent mono-layer structure. Thus it provides a good platform as a new building block for self-assembly of the noble metal Pd NCs. As shown in **Fig.2a** and **2b**, the obtained PdNCs/SnO₂-GNS nanohybrids retained a well dispersed and sheet-like morphology. It was found that small nanoparticles (black dots) were self-assembled on the surface of the SnO₂-GNS and well-distributed. The high-magnification transmission electron microscopy (HRTEM) image of PdNCs/SnO₂-GNS in **Fig.2c** shows the regular lattice spacing of 0.33 nm and 0.23 nm corresponding to those of the (110) plane of SnO_2 and (111) plane of Pd, respectively. Moreover, the inset of **Fig.2a** shows that the as-prepared PdNCs/SnO₂-GNS has a uniform and stable state existing in the aqueous solution. At the same time, the corresponding particle size distribution histograms of the Pd nanoparticles was measured and shown in **Fig.2d**.
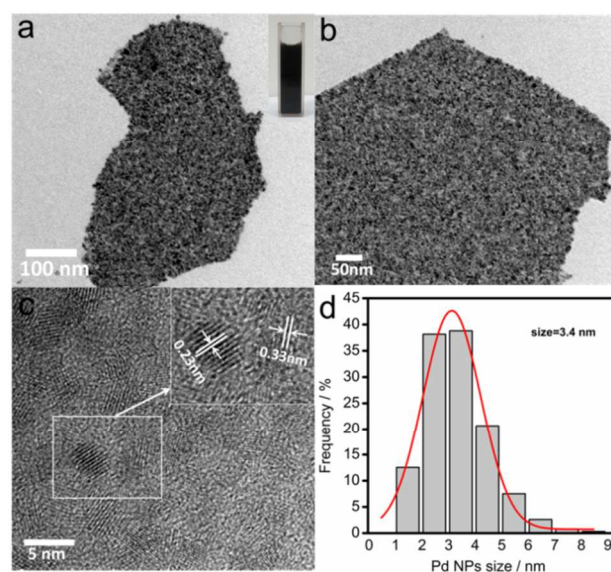
Fig.2 TEM (a, b) and HRTEM (c) images of PdNCs/SnO₂-GNS nanohybrid. The inset of (a) is the digital photo of as-made PdNCs/SnO₂-GNS has a uniform and stable state existing in the aqueous solution. (d) The corresponding particle size distribution histograms of the Pd nanoparticles.

Furthermore, the distribution of the Pd NCs supported on SnO₂-decorated GNS could be further elucidated by HAADF-STEM and the elemental mapping. The images of C, O, Sn and Pd of the PdNCs/SnO₂-GNS are shown in **Fig.3**, which were well agreed with the energy-dispersive X-ray (EDX) analysis (**Fig.S3**) (The Cu element in the EDX originates from the carbon copper

grid). It can be clearly seen that the Sn-L and Pd-L element were uniformly distributed in mono-layer GNS like a "maple leaf", which suggests that PdNCs/SnO$_2$-GNS were well synthesized.
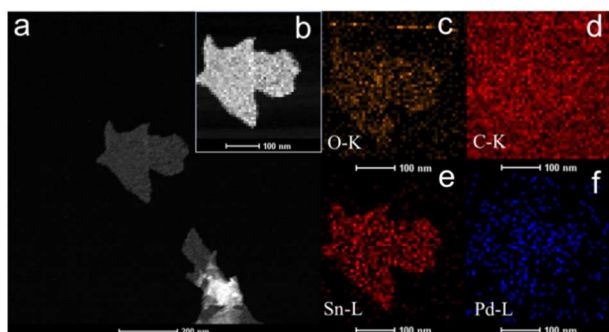
Fig.3 HAADF-STEM (a, b) and elemental mapping images (c–f) of PdNCs/SnO$_2$-GNS nanohybrid.

In order to further illustrate the composition of the PdNCs/SnO$_2$-GNS, X-ray photoelectron spectroscopy (XPS) was performed and shown in **Fig.4**. The XPS analysis confirms the existence of C, O, N, Sn, Pd3d$_{5/2}$ and Pd3d$_{3/2}$ in the PdNCs/SnO$_2$-GNS, which were well agreed with the EDX and elemental mapping analysis. Compared with the C1s XPS spectra of GO (**Fig.S4a**), the PdNCs/SnO$_2$-GNS (**Fig.4a**) display significantly decreased peak intensities of oxygenated carbon species, which further manifest the reduction of GO. **Fig.4b** shows the N1s which is ascribed to polyelectrolyte PDDA. The Pd 3d XPS spectrum in **Fig.4c** consists of two typical peaks at around 338.2 eV and 342.7 eV, corresponding to the Pd3d$_{5/2}$ and Pd3d$_{3/2}$, respectively. In the Sn 3d spectrum (**Fig.4d**), two symmetrical peaks centered at 495.2eV and 486.8eV are corresponding to Sn3d$_{5/2}$ and Sn3d$_{3/2}$ spectra, which are attributed to Sn^{4+} species. It clearly indicated the successful modification of SnO$_2$ on the surface of GNS. The presence of SnO$_2$ can be further confirmed by the O 1s XPS peak at 530.5 eV (**Fig.S4b**), which corresponds to the oxygen species in the SnO$_2$.
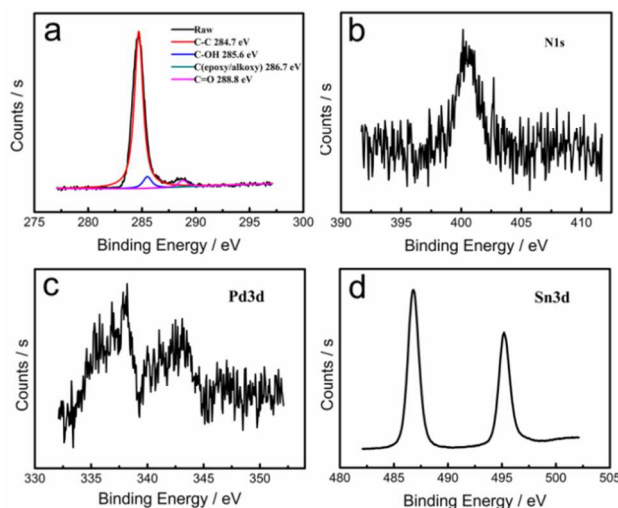
Fig.4 (a) C1s (b) N1s (c) Pd3d and (d) Sn3d XPS spectra of the PdNCs/SnO$_2$-GNS nanohybrid.

It is necessary to discuss the significant role of poly

(diallyldimethylammonium chloride) (PDDA) in this study. PDDA is a kind of water-soluble cationic polyelectrolyte attributed to ammonium group and can provide the positive charge site to attract the negatively charged PdCl$_4^{2-}$ ion *via* the electrostatic interaction. It also acts as "glue" to bind the Pd NCs upon redox reaction *in situ* growing on the surface of SnO$_2$-GNS. The zeta potential of GO and SnO$_2$-GNS can also distinctly reflect the surface charge. Compared with the zeta potential of GO (-22.0 mV), that of the as-prepared SnO$_2$-GNS dramatically changed from negative to positive value (+23.3 mV) after introduction the PDDA. To a certain extent, PDDA can create a strong electrostatic repulsion ''environment'' surrounding the noble metal Pd NCs,[47, 48] which is like a "spacer" that makes the nanosheet structure of graphene well dispersed in aqueous medium. Another control experiment was carried out under the same conditions without introduction of PDDA, which resulted in the aggregation of SnO$_2$-GNS due to absence of the electrostatic repulsion and the weak interactions in solution (**Fig.S5**). From **Fig.S5b**, it is also clearly seen that the suspension of SnO$_2$-GNS obviously aggregated in the quartz cuvette. Therefore, it is reasonable to conclude that PDDA plays a key role in attracting the precursor of Pd NCs and their self-assembly on the surface of SnO$_2$-GNS and makes PdNCs/SnO$_2$-GNS well-dispersed in aqueous by π-π interaction and electrostatic interaction.

3.2 Evaluation of catalytic activity

The catalytic activity of the as-prepared PdNCs/SnO$_2$-GNS composite material was evaluated in terms of the reduction of 4-NP into 4-AP with an excess NaBH$_4$ in aqueous solution. To our knowledge, this reaction is a typical hydrogenation reactions.[21] **Fig.5a** shows the time-dependent UV-vis spectra for the catalytic reduction of 4-NP by NaBH$_4$ over high performance Pd NCs supported on SnO$_2$-GNS. The characteristic absorption peak of 4-NP at λ_{max}=400 nm is found to gradually decreased as a function of time, accompanying by the appearance of the fresh-generated peak at 300 nm corresponding to 4-AP, which indicated the successful conversion of 4-NP to 4-AP. Simultaneously, the color of reaction system changed from light yellow to yellow-green due to the production of p-nitrophenolate ions after addition of sodium borohydride. The process of catalytic reduction was monitored very quickly within 0 to 0.5min. In **Fig.5a**, as time going on, the process gradually slowed down, until the reaction finished within 3.5 min. Based on the fact, it is found that the reduction started immediately after the addition of the catalyst and there was no induction time. The sodium borohydride is excessive during the whole process of this reaction, so the reaction can be assumed as the first-order kinetics reaction.[29, 49] And, the kinetic equation of this catalytic reaction could be shown as following:

$$-dC_t/dt = k_{app}C_t = k_{nor}c_{Pd}C_t$$

Where C_t is the concentration of 4-NP at time t. c_{Pd} (mM) is the concentration of Pd presented in the system. Then, k_{app} is the apparent reaction rate constant, which can be obtained from the slope of the linear correlation. In most of the cases, k_{app} was normalized to the c_{Pd}, deriving k_{nor} to reveal the intrinsic catalytic activity of the catalyst.

$$k_{nor} = k_{app}/c_{Pd}$$

Fig.5b shows C_t/C_0 *versus* the reaction time for the reduction of 4-NP over the catalyst-free, mono-SnO$_2$-GNS, Pd-GNS and as-prepared PdNCs/SnO$_2$-GNS. As shown in the **Fig.5b**, it is learned that catalytic efficiency in the catalyst-free or in the presence of SnO$_2$-GNS display none catalytic activity. When Pd-GNS was added into the aqueous mixture of 4-NP and NaBH$_4$ alone, the reaction was found to finish in 10 minutes. However, with the addition of highly efficient Pd nanocrystals supported on SnO$_2$-GNS, 4-NP was rapidly reduced within 3.5 min. It means that

PdNCs/SnO$_2$-GNS exhibits highly catalyze efficiency towards the reduction of nitro aromatic compounds. **Fig.5c** shows the relationship between $\ln(A_t/A_0)$ (corresponding to $\ln(C_t/C_0)$) and C_t/C_0 *versus* the reaction time t, in which A_t and A_0 are corresponding to the absorbance values at specific time intervals and initial time, respectively. The curve of $\ln(C_t/C_0)$ as function of t is found to be linear with a calculated kinetic constant k_{app} 2.03×10^{-2} s^{-1}, which was much higher than most of the other building blocks to the supported Pd nanocatalyst previously reported.[22, 23, 25, 33-36] (see **Table 1**)
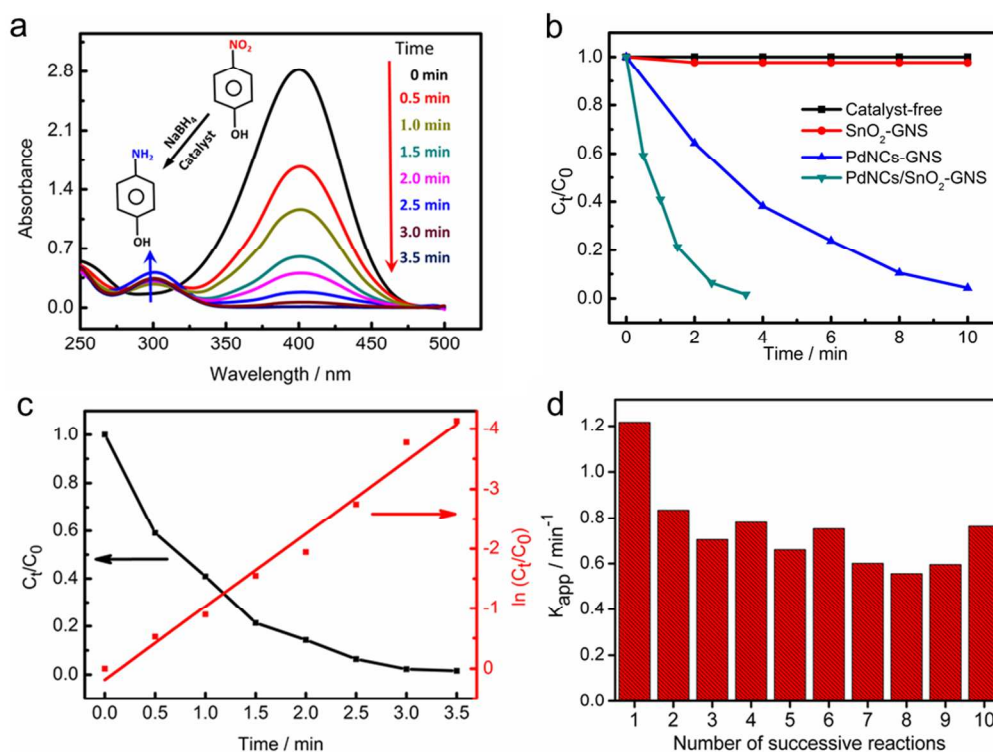
Fig. 5 (a) Time-dependent UV-vis absorption spectra for the catalytic reduction of 4-NP by NaBH$_4$ over high performance PdNCs/SnO$_2$-GNS (b) C_t/C_0 against reaction time for the reduction of 4-NP at different catalysts, which have catalyst-free, SnO$_2$-GNS, PdNCs-GNS and PdNCs/SnO$_2$-GNS, respectively. (c) C_t/C_0 and $\ln(C_t/C_0)$ against reaction time for the reduction of 4-NP by NaBH$_4$ over PdNCs/SnO$_2$-GNS. C$_0$ stands for the intensity of the absorption at 400 nm initially and C$_t$ was the absorption peak at time t. (d) k_{app} against the number of successive reaction employing high performance PdNCs/SnO$_2$-GNS nanohybrid.

Our results were also compared with reports in the literature in **Table 1**. In order to further prove the excellent catalytic performance of as-synthesized PdNCs/SnO$_2$-GNS nanohybrid, similar size of Pd NCs was chosen as the counterparts in the control experiment. Furthermore, c_{Pd} (mM L^{-1}) has been applied as the same comparison concentration of Pd presented in the system to arrive at a meaningful comparison. The content of Pd in this study is 0.02988mg mL^{-1}, which was accurately determined by ICP atomic spectrum measurement. The turnover frequency (TOF) of catalyst, which is defined as moles of reduced 4-NP per mole of Pd per second, is a very important parameter that is often used for comparing efficiency of catalyst. Some data of k_{nor} and TOF were not given in literatures. The as-prepared PdNCs/SnO$_2$-GNS showed excellent catalytic activity for reduction of 4-NP. It has the highest k_{nor} (44.91 s^{-1} mM^{-1}) and the highest TOF (1.70 s^{-1})

among the Pd catalysts loaded on a variety of supports (Fe$_3$O$_4$/graphene,[25] SnO$_2$/polyaniline,[33] SBA15,[22] carbon nanotubes,[34] ZnO,[35] Al$_2$O$_3$[23] and microgel coated polystyrene (Pd/microgel-PS)[36]). It is obviously learned that the value of TOF of Pd NCs loading on SnO$_2$-GNS (1.70s^{-1}) is much higher than that of Fe$_3$O$_4$/graphene (1.471s^{-1}), which indicated that the deposition of SnO$_2$ on GNS exhibited an excellent synergistic effect. Although the Pd NCs deposited on spherical polyelectrolyte brushes (Pd/SPB-PS) exhibits a higher k_{nor} (12.0 s^{-1} mM^{-1}), it's TOF (0.228 s^{-1}) is still lower than that of the as-prepared PdNCs/SnO$_2$-GNS. The above results clearly show that this PdNCs/SnO$_2$-GNS composite hybrid obtained in our study demonstrates preferable catalytic ability comparing with previously reported analogues.

Table 1 Comparison of normalized rate constants (k_{nor}) and TOF of high performance Pd NCs loaded on different supports for reduction 4-NP

Samples	Pd NPs size (nm)	$c_{(4-NP)}$[a] (mM)	c_{Pd} (mM)	Pd/4-NP (mol%)	k_{app}[b] (10^{-3} s^{-1})	k_{nor}[c] (s^{-1} mM^{-1})	TOF[d] (s^{-1})	Reference
PdNCs/SnO$_2$-GNS	~3.4	0.161	0.00452	0.28%	20.3	44.91	1.70	This work
Pd/Fe$_3$O$_4$/graphene	~5	1.85	0.0314	1.70%	0.061	1.943	1.471	25
Pd/SnO$_2$/polyaniline	~3.0	0.227	0.0166	7.31%	26.9	1.62	0.137	33
Pd/SBA15	~7	0.1	0.0629	62.89%	11.8	0.188	0.0053	22
Pd/oMWCNT	—	0.095	1.410	148%	—	—	0.07	34
Pd/ZnO	2.3	10	3.050	30.5%	—	—	0.00025	35
Pd/Al$_2$O$_3$	>5.8	0.1	0.00848	8.48%	9.2	1.085	—	23
Pd/microgel-PS	3.8±0.6	0.1	0.00215	2.15%	1.5	0.698	—	36
Pd/SPB-PS	2.4±0.5	0.1	0.000366	0.366%	4.41	12.0	0.228	36

[a] c: concentration. [b] k_{app}: apparent rate constant. [c] k_{nor}: rate constant normalized to the molar concentration of Pd. [d] Data were given or calculated in the respective papers; some data were not obtained

It is well known that, the noble metal Pd NCs is favorite material for many researchers due to its unique properties in catalysis field.[25,50] Undoubtedly, this PdNCs/SnO$_2$-GNS with excellent catalytic performance for reduction of 4-NP should become a promising candidate for potential applications. However, in order to prove that the PdNCs/SnO$_2$-GNS also possess good potential in commercial fields, further research are need to investigate its catalytic stability and anti-poisoning capability. **Fig.5d** shows the values of k_{app} *versus* the number of successive reaction when employing the PdNCs/SnO$_2$-GNS as the catalyst. As shown in the image, the catalytic activity begins to decline after the first reaction and retains almost the same catalytic activity for nine rounds of reaction. Namely, it shows an excellent stability against poisoning in the reaction system.

The insight of mechanism for a reaction could always facilitate overcoming of the demerits. According to previous reports in the literature from Xia's group, we know that the poison of the catalyst may be caused by adsorption of the reaction product, 4-AP, on the surface of Pt NCs. In order to avoid this, the combinations of Pt NCs with CeO$_2$ has be applied for effectively inhibit this kind of poisoning process.[26] Hence, it can be assumed that in our study the supporting material SnO$_2$-GNS plays a significant role which is similar to CeO$_2$ for efficient avoiding poison of the catalyst. In addition, PdNCs/SnO$_2$-GNS obtained could be very easily separated through centrifugation and exhibited good recyclability.

4. Conclusion

In summary, a kind of hybrid composite material PdNCs/SnO$_2$-GNS has been successfully prepared *via* a simple approach, in which ultra-small Pd NCs with the size of 3.4 nm was uniformly distributed on the SnO$_2$-decorated GNS. The as-prepared PdNCs/SnO$_2$-GNS nanohybrid exhibited excellent catalytic activity and high cycle stabilization against poisoning for organic aromatic compound degradation. The excellent catalytic activity should arise from the following factors: (i) the ultra-small size of Pd NCs contributes a lot to the high performance of catalytic activity; (ii) SnCl$_2$ acts not only the reducing agent for graphene, but also a precursor of SnO$_2$. It could be assumed that SnO$_2$ on the GNS surface acts as "linker" (anchoring sites) for Pd NCs and they are beneficial to restricting the Pd NCs migration. Moreover, SnO$_2$ can also increase the catalytic activity of Pd NCs and demonstrates the synergistic effect between Pd NCs and SnO$_2$;

(iii) SnO$_2$-GNS shows high absorption ability towards the precursor of Pd NCs after the PDDA noncovalently functionalization, which can efficiently prevent the PdNCs/SnO$_2$-GNS from serious aggregation; It is expected that PdNCs/SnO$_2$-GNS nanohybrid might be a kind of promising candidate for potential applications such as electrocatalysis, biosensors, energy conversion in the future study.

Acknowledgements

Notes

[a] State Key Laboratory of Electroanalytical Chemistry, c/o Engineering Laboratory for Modern Analytical Techniques, Changchun Institute of applied Chemistry, Chinese Academy of Sciences, Changchun, 130022, Jilin, China. Fax: +8643185262800; Tel: +8643185262425; E-mail: dxhan@ciac.ac.cn
[b] University of Chinese Academy of Sciences, Beijing 100039, China

References

1. Y. C. Chang and D. H. Chen, *Journal of hazardous materials*, 2009, **165**, 664-669.
2. S. A. Misal, D. P. Lingojwar, M. N. Lokhande, P. D. Lokhande and K. R. Gawai, *Biotechnology letters*, 2013, 1-5.
3. A. Chinnappan and H. Kim, *RSC Advances*, 2013, **3**, 3399-3406.
4. F. Wu, L.-G. Qiu, F. Ke and X. Jiang, *Inorganic Chemistry Communications*, 2013.
5. J. Li, C.-y. Liu and Y. Liu, *Journal of Materials Chemistry*, 2012, **22**, 8426.
6. S. Saha, A. Pal, S. Kundu, S. Basu and T. Pal, *Langmuir : the ACS journal of surfaces and colloids*, 2009, **26**, 2885-2893.
7. N. P. Cheval, A. Dikova, A. Blanc, J. M. Weibel and P. Pale, *Chemistry*, 2013, **19**, 8765-8768.
8. C. A. Schoenbaum, D. K. Schwartz and J. W. Medlin, *Journal of Catalysis*, 2013, **303**, 92-99.
9. F. S. Han, *Chemical Society reviews*, 2013, **42**, 5270-5298.
10. A. Ollagnier, A. Fabre, T. Thundat and E. Finot, *Sensors and Actuators B: Chemical*, 2013, **186**, 258-262.
11. R. Bhandari and M. R. Knecht, *ACS Catalysis*, 2011, **1**, 89-98.
12. Y. J. Lee, Y. Lee, D. Oh, T. Chen, G. Ceder and A. M. Belcher, *Nano letters*, 2010, **10**, 2433-2440.
13. Y. J. Lee, H. Yi, W. J. Kim, K. Kang, D. S. Yun, M. S. Strano, G. Ceder and A. M. Belcher, *Science*, 2009, **324**, 1051-1055.

Journal of Materials Chemistry A Accepted Manuscript

14. Y. Zhao, L. Zhan, J. Tian, S. Nie and Z. Ning, *Electrochimica Acta*, 2011, **56**, 1967-1972.
15. S. Zhang, Y. Shao, H.-g. Liao, J. Liu, I. A. Aksay, G. Yin and Y. Lin, *Chemistry of Materials*, 2011, **23**, 1079-1081.
16. R. N. Singh and R. Awasthi, *Catalysis Science & Technology*, 2011, **1**, 778.
17. L. Gao, W. Yue, S. Tao and L. Fan, *Langmuir : the ACS journal of surfaces and colloids*, 2013, **29**, 957-964.
18. J. R. Chiou, B. H. Lai, K. C. Hsu and D. H. Chen, *Journal of hazardous materials*, 2013, **248-249**, 394-400.
19. S. Bai, X. Shen, G. Zhu, A. Yuan, J. Zhang, Z. Ji and D. Qiu, *Carbon*, 2013, **60**, 157-168.
20. T. R. Mandlimath and B. Gopal, *Journal of Molecular Catalysis A: Chemical*, 2011, **350**, 9-15.
21. N. Meir, I. Jen-La Plante, K. Flomin, E. Chockler, B. Moshofsky, M. Diab, M. Volokh and T. Mokari, *Journal of Materials Chemistry A*, 2013, **1**, 1763.
22. J. Morère, M. J. Tenorio, M. J. Torralvo, C. Pando, J. A. R. Renuncio and A. Cabañas, *The Journal of Supercritical Fluids*, 2011, **56**, 213-222.
23. S. Arora, P. Kapoor and M. L. Singla, *Reaction Kinetics, Mechanisms and Catalysis*, 2010.
24. H. Zhang, X. Li and G. Chen, *Journal of Materials Chemistry*, 2009, **19**, 8223.
25. X. Li, X. Wang, S. Song, D. Liu and H. Zhang, *Chemistry*, 2012, **18**, 7601-7607.
26. T. Yu, J. Zeng, B. Lim and Y. Xia, *Advanced materials*, 2010, **22**, 5188-5192.
27. P. Zhang, C. Shao, Z. Zhang, M. Zhang, J. Mu, Z. Guo and Y. Liu, *Nanoscale*, 2011, **3**, 2943-2949.
28. Y. Fang and E. Wang, *Nanoscale*, 2013, **5**, 1843-1848.
29. S. Wunder, F. Polzer, Y. Lu, Y. Mei and M. Ballauff, *The Journal of Physical Chemistry C*, 2010, **114**, 8814-8820.
30. C. Zhu, P. Wang, L. Wang, L. Han and S. Dong, *Nanoscale*, 2011, **3**, 4376-4382.
31. C. Zhu, Y. Fang, D. Wen and S. Dong, *Journal of Materials Chemistry*, 2011, **21**, 16911.
32. H. Song, L. Zhang, C. He, Y. Qu, Y. Tian and Y. Lv, *Journal of Materials Chemistry*, 2011, **21**, 5972.
33. X. Lu, Y. Xue, G. Nie and C. Wang, *Catal Lett*, 2012, **142**, 566-572.
34. H. He and C. Gao, *Molecules*, 2010, **15**, 4679-4694.
35. M.-R. Kim and S.-H. Choi, *Journal of Nanomaterials*, 2009, **2009**, 1-7.
36. Y. Mei, Y. Lu, F. Polzer, M. Ballauff and M. Drechsler, *Chemistry of Materials*, 2007, **19**, 1062-1069.
37. W. S. Hummers and R. E. Offeman, *Journal of the American Chemical Society*, 1958, **80**, 1339.
38. D. Li, M. B. Muller, S. Gilje, R. B. Kaner and G. G. Wallace, *Nature nanotechnology*, 2008, **3**, 101-105.
39. F. Li, J. Song, H. Yang, S. Gan, Q. Zhang, D. Han, A. Ivaska and L. Niu, *Nanotechnology*, 2009, **20**, 455602.
40. L.-S. Zhang, L.-Y. Jiang, H.-J. Yan, W. D. Wang, W. Wang, W.-G. Song, Y.-G. Guo and L.-J. Wan, *Journal of Materials Chemistry*, 2010, **20**, 5462-5467.
41. C. N. Rao, A. K. Sood, K. S. Subrahmanyam and A. Govindaraj, *Angewandte Chemie*, 2009, **48**, 7752-7777.
42. D. Chen, H. Feng and J. Li, *Chemical reviews*, 2012, **112**, 6027-6053.
43. Y. Fang, S. Guo, C. Zhu, Y. Zhai and E. Wang, *Langmuir : the ACS journal of surfaces and colloids*, 2010, **26**, 11277-11282.
44. J.-D. Qiu, G.-C. Wang, R.-P. Liang, X.-H. Xia and H.-W. Yu, *The Journal of Physical Chemistry C*, 2011, **115**, 15639-15645.
45. C. Zhu, S. Guo, Y. Fang and S. Dong, *ACS nano*, 2010, **4**, 2429-2437.
46. K. Liu, J. Zhang, G. Yang, C. Wang and J.-J. Zhu, *Electrochemistry Communications*, 2010, **12**, 402-405.
47. H. Chen, Y. Wang and S. Dong, *Inorganic chemistry*, 2007, **46**, 10587-10593.
48. S. Zhang, Y. Shao, H. Liao, M. H. Engelhard, G. Yin and Y. Lin, *ACS nano*, 2011, **5**, 1785-1791.
49. P. Herves, M. Perez-Lorenzo, L. M. Liz-Marzan, J. Dzubiella, Y. Lu and M. Ballauff, *Chemical Society reviews*, 2012, **41**, 5577-5587.
50. M. Giovanni, H. L. Poh, A. Ambrosi, G. Zhao, Z. Sofer, F. Sanek, B. Khezri, R. D. Webster and M. Pumera, *Nanoscale*, 2012, **4**, 5002-5008.